Theoretical Study of the Mechanism of Zeolite-Catalyzed Isomerization Reactions of Linear Butenes

M. Boronat,[†] P. Viruela,[‡] and A. Corma*[,†]

Instituto de Tecnología Química UPV-CSIC, Universidad Politécnica de Valencia, av/ dels Tarongers s/n, 46022 Valencia, Spain, and Departament de Química Física, Universitat de València, c/ Dr. Moliner 50, 46100 Burjassot (Valencia), Spain

Received: August 11, 1997; In Final Form: November 11, 1997

Density functional theory is used to study the mechanism of double-bond isomerization and skeletal isomerization of linear butenes catalyzed by a protonated zeolite, which is simulated by a cluster consisting of two Si and one Al tetrahedra. The study includes complete geometry optimization and characterization of reactants, products, reaction intermediates and transition states, and calculation of the activation energies for the different processes involved. It is shown that the double bond isomerization proceeds by a concerted mechanism which does not involve the formation of either ionic or covalent alkoxy intermediates. According to this concerted mechanism, in one step the acid OH group of the zeolite protonates the double bond of adsorbed but-1-ene and the basic neighboring O atom of the cluster abstracts a hydrogen from the olefin, restoring the zeolite active site and yielding adsorbed but-2-ene. However, the mechanism of skeletal isomerization of linear butenes consists of three elementary steps: protonation of adsorbed but-1-ene to give a secondary alkoxy intermediate, conversion of the secondary alkoxy intermediate into a branched primary one through a cyclic transition state in which the transferring methyl group is halfway between its position in the linear and in the branched species, and decomposition of the primary alkoxy intermediate to give adsorbed isobutene. The activation barriers calculated for the two reactions are in good agreement with experimental data.

1. Introduction

Isobutene is an important raw material for the production of oxygenated species such as methyl *tert*-butyl ether (MTBE) and ethyl *tert*-butyl ether (ETBE), which are currently used as boosters of the octane number of reformulated gasolines.[1,2] The catalytic cracking of petroleum cannot satisfy the growing demand for isobutene, and consequently there is an increasing interest in the skeletal isomerization of the much more abundant linear butenes as a new source of this branched olefin.

Among the large variety of solid acids that have been studied as catalysts for the skeletal isomerization of *n*-butenes,[3] 10-member ring small-pore zeolites such as ZSM-23,[4] MCM-22,[5] and ferrierite[6] are the most active and selective. The reason for the high selectivity to isobutene obtained with these zeolites seems to be their pore size, which is too narrow to allow dimerization or oligomerization reactions that compete with the monomolecular skeletal isomerization of *n*-butenes. However, little more is known about the intermediates and elementary steps involved in this mechanism.

For a long time, the mechanism of heterogeneous catalysis on solid acids such as zeolites was considered to be equivalent to that of homogeneous reactions in superacid media. It was supposed that the interaction of olefins with the Brønsted acid sites of the zeolites would result in the formation of adsorbed carbenium ions, which would be the intermediate species in the acid-catalyzed cracking, isomerization, and alkylation reactions of hydrocarbons. However, except for alkyl-substituted cyclopentenyl[7] and indanyl[8] cations, in which the positive charge is delocalized and sterically inaccessible to framework oxygens, no free carbenium ions have been experimentally observed on the surface of acidic zeolites. Instead, a number of ^{13}C-NMR MAS spectroscopic studies[9−11] suggest that the intermediate species in zeolite-catalyzed reactions of hydrocarbons are alkoxy complexes, with the alkyl group covalently bonded to the zeolite framework oxygens. Similar conclusions have been obtained from quantum-chemical studies of the interaction of small olefins with the hydroxyl groups of acidic zeolites.[12,13] These studies have shown that protonation of olefins by zeolitic OH groups results in formation of stable covalent alkoxy intermediates via ionic transition states whose organic fragments have a geometry and electronic structure similar to those of classical carbenium ions.

In a previous study,[14] an ab initio quantum-chemical investigation of the mechanism of skeletal isomerization of linear butenes in superacid solution was performed, and it was found that the secondary linear 2-butyl cation is converted into the branched *tert*-butyl cation through the primary isobutyl cation, which is the transition state for the reaction. But for the reasons we have just mentioned, these results are not necessarily extrapolative to heterogeneous catalysis. When the reaction occurs in the interior of a zeolite, its mechanism may be different and should be calculated including explicitly the interactions of the organic reactants with the catalyst surface.

We present now a theoretical investigation of the mechanisms of zeolite-catalyzed double-bond isomerization and skeletal isomerization of linear butenes in which the active site of the catalyst has been simulated by a cluster consisting of two silicon and one aluminum tetrahedra. This model cluster contains both

* To whom correspondence should be addressed.
[†] Universidad Politénica de Valencia.
[‡] Universitat de Valéncia.

S1089-5639(97)02672-8 CCC: $15.00
Published on Web 01/15/1998

the Brønsted acidic hydroxyl group and one neighboring basic oxygen, and therefore, it can correctly model the bifunctional nature of the zeolite active sites. The study includes geometry optimization and characterization of reactants, products, reaction intermediates, and transition states, and calculation of the activation energies for the different processes involved.

The present investigation is based on density functional theory,[15,16] a methodology that allows for the inclusion of electron correlation at a much lower computational cost than the cost of traditional ab initio methods. This is especially important in theoretical studies of heterogeneous catalysis, where large systems are involved and electron correlation is essential for describing correctly the interactions between the organic molecules and the catalyst surface. The geometry optimizations and characterization of the stationary points have been carried out using DFT methods and afterward single-point calculations on these geometries using the correlated post-HF MP2 method have been performed.

2. Computational Details

All calculations in this work were performed on the IBM RS/6000 and SGI Power Challenge L workstations of the Departament of Química Física, Universitat de València by means of the Gaussian 94[17] computer program and, except where otherwise stated, are based on density functional theory. Recent work relative to the performance of different functionals[18] has shown that the DFT hybrid methods that include the Hartree−Fock exact exchange provide results comparable to those obtained with post-HF-correlated methods. The method used in this work combines Becke's hybrid three-parameter exchange functional[19] with the gradient-corrected correlation functional of Perdew[20] (B3P86), and it was chosen because in a previous theoretical study of the mechanism of branching rearrangement of 2-pentyl cation,[21] it was found to give the best overall performance among several DFT and ab initio methods. The standard 6-31G* basis set[22] that includes d-type polarization functions on non-hydrogen atoms and the 6-31G** basis set[23] that also includes p-type polarization functions on hydrogens were employed.

The geometries of both minima and transition states were fully optimized using the Berny analytical gradient method,[24] and all stationary points were characterized by calculating the Hessian matrix and analyzing the vibrational normal modes. Zero-point vibrational corrections (ZPE) obtained from frequency calculations were added to the total energies. When it was necessary to check which are the two minima connected by a transition state, the intrinsic reaction coordinate method[25] was used. Single-point calculations on the B3P86-optimized geometries were performed using the ab initio second-order Møller-Plesset perturbation theory[26] that takes into account the core electrons (MP2(fu)//B3P86).

The cluster used in this work to simulate the active site of the zeolite consists of one aluminum and two silicon tetrahedra whose dangling bonds, which actually connect the cluster with the rest of the solid, are saturated with hydrogen atoms: $H_3Si-OH-AlH_2-O-SiH_3$. In all calculations the heavy atoms of the cluster were constrained to be in the same plane to avoid artificial distortions that would not occur in the zeolite crystal. No other symmetry restrictions were used.

3. Results and Discussion

First of all, it is important to note that the B3P86/6-31G*-optimized geometry of the hydroxyl group of the $H_3Si-OH-AlH_2-O-SiH_3$ cluster used in this work to simulate the zeolite active site is similar to that reported by Sauer for a variety of model clusters obtained using ab-initio-correlated methods.[27] In section 3.1 we present the structures of the reactants, but-1-ene and but-2-ene, and the product, isobutene, adsorbed on the zeolite surface (see Figure 1 and Table 1). The mechanism of the double-bond migration in linear butenes is discussed in section 3.2, and the optimized geometry of the transition state for this process is shown in Figure 2. The structures of the alkoxy intermediates depicted in Figure 3 and the optimized values of their most important parameters summarized in Table 2 are analyzed in section 3.3. Finally, the complete mechanism of skeletal isomerization of linear butenes is discussed in section 3.4. The optimized geometries of the transition states for the skeletal isomerization and for the alkoxy formation from adsorbed olefins are shown in Figures 4 and 5, respectively. The relative energies of all structures with respect to the sum of the energies of the cluster and but-1-ene are given in Table 3 together with the absolute zero-point corrections and the nature of the stationary points, and Figure 6 shows the calculated potential-energy profile for the two studied reactions.

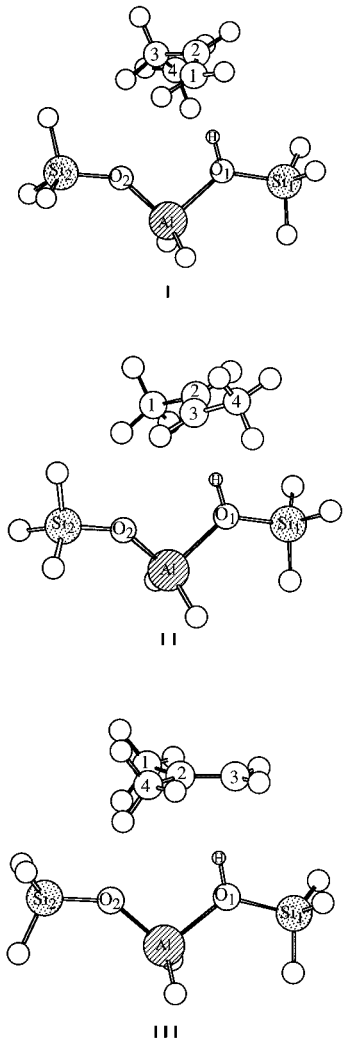

Figure 1. Calculated structures for but-1-ene (**I**), but-2-ene (**II**), and isobutene (**III**) adsorbed on the zeolite surface.

3.1. Adsorbed Olefins. Figure 1 shows the B3P86/6-31G*-calculated structures corresponding to but-1-ene (**I**), but-2-ene (**II**), and isobutene (**III**) adsorbed on the zeolite surface. In all cases, the double bond of the olefin interacts with the proton of the Brønsted acid site of the zeolite, forming a complex of π nature, in agreement with previous ab initio results.[13] The

TABLE 1: Optimized Values of the Most Important Geometric Parameters of But-1-ene (I), But-2-ene (II), and Isobutene (III) Adsorbed on the Zeolite Surface[a]

parameter[b]	I	II	III
	Distances (Å)		
$r(Al-O_1)$	1.971	1.970	1.967
$r(Al-O_2)$	1.750	1.749	1.753
$r(O_1-Si_1)$	1.703	1.702	1.704
$r(O_2-Si_2)$	1.631	1.630	1.633
$r(O_1-H)$	0.993	0.994	0.994
$r(H-C_1)$	2.042		
$r(H-C_2)$	2.294	2.162	2.262
$r(H-C_3)$		2.097	2.081
$r(C_1-C_2)$	1.340	1.497	1.500
$r(C_2-C_3)$	1.497	1.343	1.345
$r(C_3-C_4)$	1.530	1.496	
$r(C_2-C_4)$			1.500
	Angles (deg)		
$a(O_1AlO_2)$	95.9	96.3	98.0
$a(AlO_1Si_1)$	127.8	127.1	125.3
$a(AlO_2Si_2)$	144.4	146.4	140.2
$a(AlO_1H)$	114.2	114.8	118.4

[a] The optimized values for isolated olefins are the following: but-1-ene, $r(C_1-C_2) = 1.332$, $r(C_2-C_3) = 1.509$, $r(C_3-C_4) = 1.525$; but-2-ene; $r(C_1-C_2) = r(C_3-C_4) = 1.495$, $r(C_2-C_3) = 1.334$; isobutene: $r(C_1-C_2) = r(C_2-C_4) = 1.502$, $r(C_2-C_3) = 1.335$. [b] The atomic numbering is given in Figure 1.

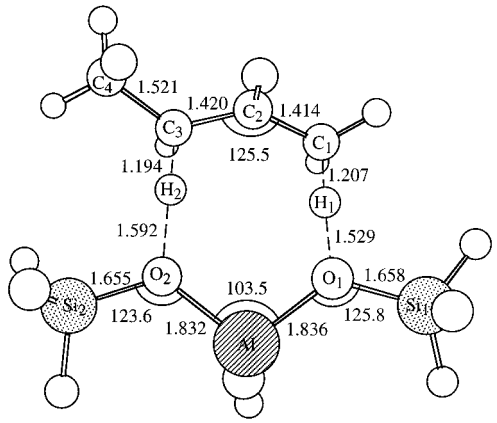

IV

Figure 2. B3P86/6-31G*-optimized geometry of the transition state for the double-bond isomerization in linear butenes (**IV**). Distances are in angstroms and angles in degrees.

optimized values of the most important geometric parameters of structures **I**−**III** are summarized in Table 1. In the three complexes formed, the hydrogen atom of the bridging hydroxyl group of the cluster is nearly equidistant from the two carbon atoms of the double bond, being all calculated $H_{hydroxyl}-C_{double\ bond}$ distances between 2.0 and 2.3 Å. The C−C bond lengths and CCC angles of the three adsorbed olefins are equivalent to those calculated for the isolated molecule at the same level of theory, and the main changes observed in the cluster geometry by formation of the complexes are those related to the orientation of the proton of the OH group toward the double bond of the olefin. The $Al-O_1$ bond length decreases about 0.2 Å, while the O_1-H_1 bond length increases in the same quantity. The AlO_1Si_1 angle closes from 139.9° to 125−128° and the O_1AlO_2 and AlO_1H_1 angles open from 86.1° to 96−98° and from 98.7° to 114−118°, respectively.

The three π complexes have been characterized by frequency calculations. One imaginary vibration mode of 32i cm^{-1} and one of 41i cm^{-1} have been obtained for the complexes formed by but-1-ene (**I**) and but-2-ene (**II**), respectively, and three

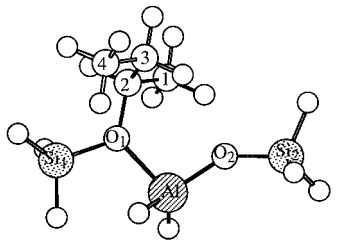

V

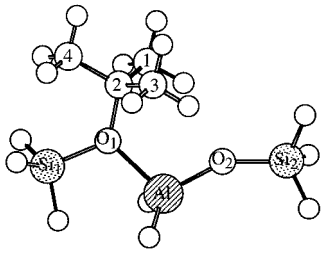

VI

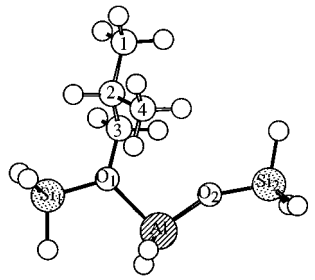

VII

Figure 3. Calculated structures for the secondary (**V**), tertiary (**VI**), and primary (**VII**) alkoxy intermediates.

TABLE 2: Optimized Values of the Most Important Geometric Parameters of the Secondary (V), Tertiary (VI), and Primary (VII) Alkoxy Intermediates

parameter[a]	V	VI	VII
	Distances (Å)		
$r(Al-O_1)$	1.996	2.021	1.993
$r(Al-O_2)$	1.741	1.742	1.739
$r(O_1-Si_1)$	1.707	1.710	1.707
$r(O_2-Si_2)$	1.630	1.630	1.628
$r(O_2-C_2)$	1.477	1.497	
$r(O_2-C_3)$			1.459
$r(C_1-C_2)$	1.514	1.521	1.529
$r(C_2-C_3)$	1.519	1.520	1.521
$r(C_3-C_4)$	1.524		
$r(C_2-C_4)$		1.523	1.526
	Angles (deg)		
$a(O_1AlO_2)$	102.5	104.6	98.6
$a(AlO_1Si_1)$	115.6	110.2	117.9
$a(AlO_2Si_2)$	149.8	151.2	154.2
$a(AlO_2C)$	127.0	124.6	121.5

[a] The atomic numbering is given in Figure 3.

imaginary frequencies of 43i, 24i, and 13i cm^{-1} have been found for the isobutene π complex (**III**). All these small imaginary vibration modes are associated either with breaking of the symmetry plane in which the heavy atoms of the cluster are constrained or with rotation of the hydrogen terminations of

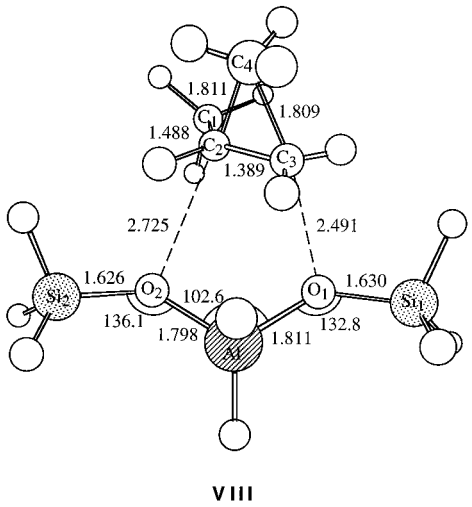

VIII

Figure 4. B3P86/6-31G*-optimized geometry of the transition state for the skeletal isomerization of butenes (**VIII**). Distances are in angstroms and angles in degrees.

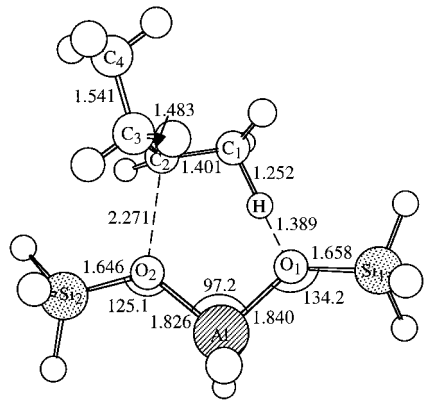

IX

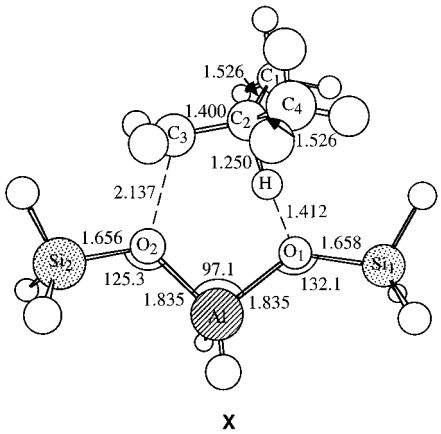

X

Figure 5. B3P86/6-31G*-optimized geometry of the transition states for alkoxide formation from adsorbed but-1-ene (**IX**) and isobutene (**X**). Distances are in angstroms and angles in degrees.

the silicon atoms, and consequently, the three structures have been characterized as minima on the potential-energy surface.

The adsorption energies of the three butenes, calculated as the difference between the total energy of the complex and the sum of the energies of the cluster and the isolated olefin, are very similar. The B3P86/6-31G* values are 7.1, 7.2, and 7.6 kcal/mol for but-1-ene, but-2-ene and isobutene, respectively, and when the zero-point correction is included, they are slightly lower—6.1, 6.3, and 6.9 kcal/mol, respectively. The MP2(fu)/6-31G*//B3P86/6-31G*-calculated values are slightly higher than the DFT ones (10.3 kcal/mol for but-1-ene, 10.5 kcal/mol for but-2-ene, and 10.7 kcal/mol for isobutene) and also nearly equivalent for the three systems. From the relative energies listed in Table 3 it can also be observed that the complexes formed by but-2-ene (structure **II**) and isobutene (structure **III**) are about 3−5 kcal/mol more stable than that formed by but-1-ene (structure **I**), which is approximately of the order of stability of the three isolated olefins. Finally, it has been found that the net charges on the most important atoms of the three π complexes hardly vary with respect to those of the isolated butenes and cluster, and consequently, only a small increase of about $+0.08e$ in the total charge of the olefins is produced by adsorption on the catalyst.

TABLE 3: B3P86/6-31G*-Calculated Relative, Zero-Point (ZPE) and Zero-Point-Corrected Relative Energies (in kcal/mol), Nature of the Stationary Points and MP2(fu)/6-31G*//B3P86/6-31G* Calculated Relative Energies (in kcal/mol)[b]

structure	E_{rel}	ZPE_{abs}	$(E + ZPE)_{rel}$	nature	MP2//DFT$_{rel}$
cluster + but-1-ene[a]	0.0	121.7	0.0	MIN	0.0
cluster + but-2-ene	−3.8	121.4	−4.1	MIN	−3.0
cluster + isobutene	−4.1	121.3	−4.4	MIN	−3.9
I	−7.1	122.6	−6.1	MIN	−10.3
II	−11.0	122.3	−10.4	MIN	−13.5
III	−11.7	122.1	−11.3	MIN	−14.6
IV	16.1	119.5	14.0	TS	24.1
V	−23.9	125.1	−20.4	MIN	−26.3
VI	−23.7	124.8	−20.5	MIN	−27.2
VII	−22.3	125.2	−18.8	MIN	−24.3
VIII	33.5	122.2	34.1	TS	32.8
IX	13.1	120.7	12.1	TS	18.1
X	19.7	120.5	18.6	TS	23.2

[a] The total energies computed for the cluster and for isolated but-1-ene are −978.591 846 and −157.800 692 hartrees, respectively, at the B3P86/6-31G* level and −975.447 671 and −156.640 075 hartrees, respectively, at the MP2(fu)/6-31G*//B3P86/6-31G* level. [b] The sum of the energies of the cluster and isolated but-1-ene is taken as the energy origin.

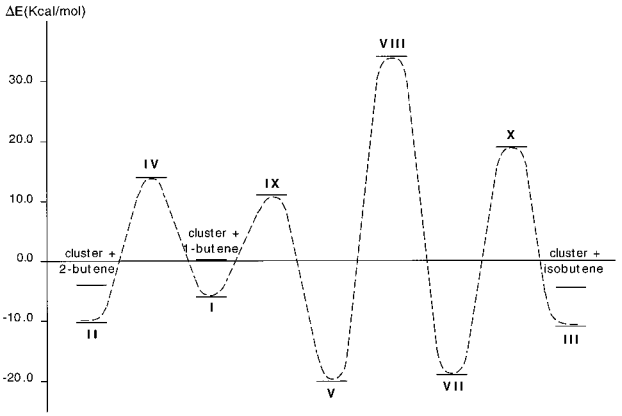

Figure 6. B3P86/6-31G* potential-energy profile for the double-bond isomerization and the skeletal isomerization of linear butenes. The sum of the energies of the cluster and isolated but-1-ene is taken as the origin of energies.

3.2. Double-Bond Isomerization. The double-bond migration in linear alkenes is a very fast process that requires relatively weak acid sites, and it is usually accompanied by skeletal isomerization, oligomerization, or cracking reactions. To explain how the double-bond isomerization occurs on solid acids such as zeolites, Kazansky[28] has proposed a mechanism that involves the formation of a surface alkoxy group by proton

addition from the zeolite to the olefin double bond followed by decomposition of this alkoxy intermediate. However, our results for the conversion of but-1-ene into but-2-ene catalyzed by a zeolite indicate that this reaction proceeds by a concerted mechanism that does not involve the formation of either ionic or covalent alkoxy intermediates.

To check whether inclusion of polarization functions on the hydrogen atoms has some effect on the geometries or energetics of this type of process, we have studied the mechanism of the double-bond migration in linear butenes using both the 6-31G* and the 6-31G** basis sets, but since no important differences between the results provided by the two methods were observed, the rest of the study was performed using only the smaller 6-31G* basis set.

Figure 2 shows the optimized geometry of the transition state obtained for this process: structure **IV**. In this structure there are two hydrogen atoms, H_1 and H_2, situated between one oxygen atom of the cluster and one carbon atom of the migrating double bond, the two C−H−O angles being approximately 180°. The C_1-H_1 and C_3-H_2 bond lengths are shorter than the H_1-O_1 and H_2-O_2 distances, and the C_1-C_2 and C_2-C_3 bond lengths are similar and between those calculated for single (∼1.50 Å) and for double (∼1.33 Å) C−C bonds. The Mulliken population analysis indicates that transition state **IV** has ionic character. The positive charge on the C_4H_9 fragment is important, +0.617*e*, and it is mainly localized on C_2. The net atomic charges on H_1 and H_2 are between those of the hydrogen atoms bonded to carbon atoms (about +0.20*e*) and that of the proton of the cluster hydroxyl group (+0.478*e*). The negative charge on the cluster is symmetrically distributed between the two oxygen atoms, and this charge delocalization is clearly reflected in the optimized geometry. The two Al−O bond lengths are similar (1.832−1.836 Å), and the same is observed for the two Si−O distances (1.655−1.658 Å) and for the two AlOSi angles (124−126°).

Three imaginary vibration modes have been obtained from the frequency calculations performed for structure **IV**. Two of them, of 35i and 8i cm^{-1}, are associated with the movement of the AlH_2 group out of the plane containing the heavy atoms of the cluster and with rotation of the SiH_3 groups, respectively. Since they are small in magnitude and are not related to the reaction coordinate, they have not been considered in the characterization of the stationary point. The most important imaginary vibration frequency, 400i cm^{-1}, is associated with the movement of the hydrogen atoms H_1 and H_2 between the oxygen atoms O_1 and O_2 of the cluster and the carbon atoms C_1 and C_3 of the olefin and has allowed us to characterize structure **IV** as the transition state for this reaction. This reaction coordinate corresponds to a concerted mechanism in which the bifunctional nature of the zeolite active sites is made patent. In one step, the H_1 of the acid hydroxyl group of the zeolite protonates the C_1 atom of the double bond of adsorbed but-1-ene, and simultaneously, the neighboring basic O_2 of the zeolite abstracts a hydrogen atom, H_2, from the carbon atom C_3, restoring the catalyst active site and yielding adsorbed but-2-ene.

The real activation barrier for this reaction should be calculated as the energy difference between transition state **IV** and adsorbed but-1-ene **I**. However, to compare with experimental information, the apparent activation energy with respect to the separated reactants, which are isolated but-1-ene and the model cluster, has been calculated. It can be observed in Table 3 that there is a very good agreement between the values calculated assuming this concerted mechanism (16.1 and 14.0 kcal/mol with the ZPE correction) and the experimental activation energies of double-bond isomerization reactions in zeolites, which are of the order of 15−20 kcal/mol.[28,29] Finally, the MP2(fu)/6-31G*//B3P86/6-31G*-calculated activation energy, 24.1 kcal/mol, is too high in relation to the experimental data and also with respect to the DFT results. This tendency of DFT-based methods to afford activation barriers lower than those provided by ab initio methods in which electron correlation is approximately taken into account has already been reported in several comparative studies of organic reactions.[30] It has been argued that more extensive CI calculations probably would provide activation barriers in closer agreement with those obtained using DFT-based methods.[30a]

3.3. Reaction Intermediates. Since in our previous work concerning the mechanism of skeletal isomerization of linear butenes in superacid media it was found that the secondary 2-butyl and the tertiary *tert*-butyl cations were the reactant and the reaction product, respectively, and that the primary isobutyl cation was the transition state for the process, we have tried to localize these three carbenium ions adsorbed on the zeolite surface. The optimized geometries of the secondary (structure **V**), tertiary (structure **VI**), and primary (structure **VII**) "adsorbed carbenium ions" given in Figure 3 and Table 2, and the Mulliken population analysis indicate that these species are not ionic but correspond to covalently bonded alkoxy complexes, in agreement with previous ab initio results.[12,13]

The optimized C−C bond lengths of structures **V**−**VII**, all of them between 1.51 and 1.53 Å, are equivalent to those calculated for saturated alkanes at the same level of theory, 1.527 Å for isobutane and 1.524 and 1.526 Å for *n*-butane. The three calculated C−O bond lengths are typical of covalent organic compounds, such as esters and alcohols, and increase from 1.459 Å in structure **VII** to 1.477 Å in **V** and 1.497 Å in **VI**, probably owing to steric factors. This elongation of the C−O bond produces a slight increase in the net atomic charge on the involved carbon atom when passing from the primary (qC_3 = −0.083*e*) to the secondary (qC_2 = +0.083*e*) and the tertiary (qC_2 = +0.278*e*) alkoxy complexes. Nevertheless, the total positive charges on the three butyl fragments are similar and low (about +0.4*e*) and are mainly localized on the carbon atoms bonded to oxygen. The most important changes observed in the geometry of the catalyst active site mainly affect the angles around the O atom bonded to the alkyl group, with experiment variations of up to 30° in order to accept the more voluminous C_4H_9 fragments.

The calculated energies for the three complexes given in Table 3 are similar. The B3P86/6-31G* relative energies of structures **V**−**VII** with respect to the cluster and but-1-ene are 23.9, 23.7, and 22.3 kcal/mol, respectively, and when the zero-point correction is included, the tertiary complex becomes 0.1 kcal/mol more stable than the secondary one, while structure **VII** continues being only 1.6 kcal/mol less stable. When the MP2-(fu)/6-31G* ab initio method is used, the relative energies of the three complexes are lowered by 2−3 kcal/mol, the tertiary complex **VI** being 1 kcal/mol more stable than the secondary **V** and the primary one **VII** being 2 kcal/mol less stable. This energetic uniformity also indicates the covalent nature of the alkoxy complexes because when their ionic character is increased by elongating the C−O bond, differences in stability between them appear. To prove this, three calculations have been carried out at the B3P86/6-31G* level in which the C−O distance has been held fixed at a value of 2.2 Å while all other parameters have been allowed to fully optimize. The positive charge on the C_4H_9 fragments of the resulting structures has

been increased to about +0.6*e*, the C−C bond lengths and CCC angles are more similar to those of free carbenium ions, and the three structures have been greatly destabilized. The relative energy of the tertiary "stretched" complex with respect to the cluster and but-1-ene is 0.3 kcal/mol, and the secondary and primary complexes are 6.6 and 15.4 kcal/mol, respectively, less stable than the tertiary one.

The three alkoxy complexes have been characterized as minima on the potential-energy surface, since the imaginary vibration modes obtained from frequency calculations (one of 22i cm^{-1} for structure **V**, one of 47i cm^{-1} for **VI**, and two of 27i and 19i cm^{-1} for **VII**) are small in magnitude and mainly related to the breaking of the symmetry plane that contains the heavy atoms of the cluster.

3.4. Skeletal Isomerization. Structure **VIII** in Figure 4 is the transition state for the zeolite-catalyzed unimolecular skeletal isomerization of linear butenes. Unlike in superacid media, neither the optimized geometry nor the net atomic charges of this structure correspond to a primary isobutyl cation. The Mulliken population analysis indicates that **VIII** is higly ionic, the total positive charge on the C_4H_9 fragment being +0.816*e*. This charge is stabilized by the two oxygen atoms of the cluster, which are at 2.725 and 2.491 Å respectively from C_2 and C_3. The C_2-C_3 bond length, 1.389 Å, is between that corresponding to a single (∼1.50 Å) and to a double (∼1.33 Å) C−C bond. The C_2-C_4 and C_3-C_4 distances are equal and long, 1.811 and 1.809 Å, respectively, because they correspond to the two bonds that are being formed or broken during the branching isomerization reaction. The result is a structure in which the transferring methyl group is halfway between its position in the linear and in the branched species.

The reaction coordinate associated with the only imaginary vibration mode obtained from the frequency calculation, 456i cm^{-1}, is quite complicated. It is related to the breaking of one of the two C−C bonds in which C_4 is involved, to the approaching of either C_2 or C_3 to one of the oxygen atoms of the cluster, and to movements of the hydrogen atoms attached to the carbon atoms that form the cyclopropane ring. We can think of two different mechanisms that would be in agreement with this reaction coordinate. In one of them, structure **VIII** would be the transition state connecting two alkoxy intermediates. Breaking of the C_2-C_4 bond and approximation of C_2 to O_2 would result in formation of the secondary alkoxy complex **V**, while breaking of the C_3-C_4 bond and interaction of C_3 with O_1 would yield the primary complex **VII**. The other one is a concerted mechanism similar to that obtained for the double-bond isomerization, in which in the unique step of the linear olefin would be transformation into the branched one. If at the same time that the C_3-C_4 bond is broken the hydrogen atom attached to C_2 is transferred to O_2, adsorbed isobutene would be obtained. In the same way, a simultaneous breaking of the C_2-C_4 bond and migration to O_1 of one of the hydrogen atoms attached to C_3 would yield adsorbed but-2-ene. This second possibility has been ruled out by a calculation performed using the intrinsic reaction coordinate method, which indicates that transition state **VIII** connects minima **V** and **VII**, that is, the secondary and primary alkoxy intermediates. According to this, the complete mechanism of skeletal isomerization of linear butenes would consist of three elementary steps: (1) formation of the secondary alkoxide **V** by protonation of adsorbed but-1-ene **I**, (2) conversion of the secondary alkoxy intermediate **V** into the branched primary one **VII** through transition state **VIII**, and (3) decomposition of the primary alkoxide **VII** to give adsorbed isobutene **III**.

Figure 5 shows the optimized geometry of the transition states obtained for the first (structure **IX**) and third (structure **X**) steps of this mechanism. In both structures there is a hydrogen atom half-transferred between one of the oxygen atoms of the zeolite and one of the carbon atoms of the olefin double bond, while the other carbon atom of the double bond is interacting with the neighboring basic oxygen atom of the cluster.

Characterization of both stationary points by frequency calculations indicates that they are transition states because they show one important imaginary vibration mode (563i cm^{-1} for **IX** and 535i cm^{-1} for **X**) clearly associated with the movement of the hydrogen atom that is protonating the olefin or is being given back to the zeolite. For structure **IX** another imaginary vibration mode of 24i cm^{-1} associated with the movement of the AlH_2 group out of the plane containing the heavy atoms of the cluster has been obtained, but owing to its small magnitude, it has not been considered in the characterization of the stationary point. The same can be said with respect to three small imaginary frequencies related to the hydrogen terminations of the Al and Si atoms of the cluster that have been found for structure **X**.

It can be observed in Figure 5 that the optimized values of the geometric parameters involved in the reaction coordinate are similar in the two structures. The hydrogen atom that is being transferred is closer to the carbon atom of the olefin, 1.25 Å, than to the oxygen atom of the cluster, 1.389 Å in **IX** and 1.412 Å in **X**. The C_1-C_2 in **IX** and C_2-C_3 in **X** bond lengths, 1.40 Å, are between those of a double and a single C−C bond, and the two calculated $C-O_2$ distances are also similar, 2.271 Å for **IX** and 2.137 Å for **X**. In the zeolitic fragments it can be seen that all Al−O and all O−Si bond lengths are similar, about 1.66 Å for the O−Si distances and between 1.83 and 1.84 Å for the Al−O ones. The two O−Al−O angles are about 10° greater than in the isolated cluster, and the $Al-O_2-Si_2$ angles are from 150° in the isolated cluster to 125° in both transition states, reflecting the strong interaction existing between this oxygen atom and the carbon atom that will form the covalent C−O bond.

The Mulliken population analysis indicates that both transition states have ionic character. The total positive charge on the organic fragment, +0.633*e* and +0.581*e* for structures **IX** and **X**, respectively, is mainly localized on the hydrogen atom that is being transferred and on the carbon atom that is interacting with the basic oxygen atom of the cluster, while the negative charge on the zeolitic fragment is quite delocalized between the two oxygen atoms.

From the relative energies of transition states **VIII**−**X** listed in Table 3 it can be seen that the rate-determining step of the proposed mechanism is the conversion of the secondary alkoxy intermediate **V** into the primary alkoxy intermediate **VII** through transition state **VIII**, and therefore, the apparent activation energy for the skeletal isomerization of linear butenes should be calculated as the energy difference between transition state **VIII** and the separated reactants. The calculated values, 33.5 and 34.1 kcal/mol with the ZPE correction at the B3P86/6-31G* level and the MP2(fu)/6-31G*//B3P86/6-31G* value of 32.8 kcal/mol, compare well with the experimental apparent activation energy value of 30 kcal/mol measured for the unimolecular skeletal isomerization of *n*-butenes catalyzed by a zeolite.[31] However, the real activation energy of every step should be calculated as the energy difference between the transition state of the process and the minimum corresponding to the reactant. For the first step of the mechanism, protonation of adsorbed but-1-ene, the apparent activation energy is 13.1 kcal/mol, and

12.1 kcal/mol with the ZPE. By addition of the adsorption energy of but-1-ene, a real activation barrier of 20.2 kcal/mol, and 18.2 kcal/mol with the ZPE, is obtained at the B3P86/6-31G* level. The MP2(fu)-calculated apparent and real activation barriers are higher, 18.1 and 28.4 kcal/mol, respectively, as has been previously discussed. For the second and rate-determining step of the mechanism, the real activation energy is the energy difference between state **VIII** and the alkoxy intermediate **V.** The values calculated in this way are high, 57.4 kcal/mol at the B3P86/6-31G* level, 54.4 kcal/mol with the ZPE, and 59.1 kcal/mol at the MP2(fu)/6-31G*//B3P86/6-31G* level. The same occurs with the third step, decomposition of the primary alkoxy intermediate **VII** through transition state **X**. The real activation energies at the B3P86/6-31G*, B3P86/6-31G*+ZPE, and MP2(fu)/6-31G*//B3P86/6-31G* levels, 42.0, 37.4, and 47.5 kcal/mol, respectively, are much higher than the apparent values of 19.7, 18.6, and 23.2 kcal/mol. This is due to the great stability of the alkoxy intermediates, whose strong covalent C−O bond has to be broken in order for the reaction to take place, and this certainly requires a high activation energy. To avoid such high real activation barriers, several attempts have been made to find an alternative concerted mechanism in which protonation and skeletal rearrangement of the olefin occur simultaneously and in which no alkoxy intermediates are involved, but none of them has succeeded.

4. Conclusions

The mechanisms of zeolite-catalyzed double-bond isomerization and skeletal isomerization of linear butenes have been studied theoretically by means of density functional theory. The geometries of reactants, products, reaction intermediates, and transition states have been optimized within the constraints reported in the computational details section. The stationary points have been characterized by frequency calculations, and the activation barriers for the different processes considered have been calculated. Single-point calculations using the correlated ab initio MP2 method have also been performed.

It has been shown that the double-bond isomerization in linear butenes proceeds by a concerted mechanism in which the bifunctional nature of the zeolite active sites is made patent. In this mechanism neither an ionic nor an alkoxy intermediate was involved. At the same time that the acid OH group of the zeolite protonates the double bond of adsorbed but-1-ene, the neighboring basic O of the cluster abstracts a hydrogen from the olefin, restoring the zeolite active site and yielding adsorbed but-2-ene. The DFT-calculated activation energy for this process is in very good agreement with experimental reported values of 15−20 kcal/mol, while the MP2(fu)//DFT value is too high.

With respect to the reaction intermediates, we have tried to localize the 2-butyl, *tert*-butyl, and primary isobutyl cations adsorbed on the zeolite surface. Our density functional results indicate, in agreement with previous ab initio data, that these species do not exist as free carbenium ions but are covalently bonded to the zeolite framework oxygens forming very stable alkoxy complexes.

The mechanism of skeletal isomerization of linear butenes has been found to consist of three elementary steps: (1) formation of the secondary alkoxy intermediate by protonation of adsorbed but-1-ene, (2) isomerization of this linear secondary alkoxide into the branched primary one, and (3) decomposition of the primary alkoxy intermediate to give adsorbed isobutene. The geometries and energies of the transition states for the first and last steps of this mechanism are similar to those obtained using ab initio methods. The transition state for the second and rate-determining step of the mechanism has a cyclic structure in which the transferring methyl group is halfway between its position in the linear and in the branched species, and in which the positive charge is stabilized by the oxygen atoms of the zeolite. The calculated apparent activation energy for the whole process is in very good agreement with a recently determined experimental value of 30 kcal/mol.

Acknowledgment. The authors thank Centre de Informàtica and Departament de Química Física, Universitat de València for computing facilities. They thank C.I.C.Y.T. (Project MAT 94-0359) and Conselleria de Cultura, Educació i Ciència de la Generalitat Valenciana for financial support. M.B. thanks the Conselleria de Cultura, Educació i Ciència de la Generalitat Valenciana for a personal grant.

References and Notes

(1) Juguin, B.; Torck, B.; Martino, G. In *Catalysis by acids and bases*; Imelik, B., et al., Eds.; Studies Surface Science Catalysis 20; Elsevier: Amsterdam, 1985; p 253.

(2) (a) Pecci, G.; Floris, T. *Hydrocarbon Process* **1977**, *56*, 98. (b) Maxwell, I. E.; Naber, J. E. *Catal. Lett.* **1992**, *12*, 105. (c) Maxwell, I. E.; Naber, J. E.; de Jong, K. P. *Appl. Catal. A* **1994**, *113*, 153.

(3) Butler, A. C.; Nicolaides, C. P. *Catal. Today* **1993**, *18*, 443.

(4) Xu, W. Q.; Yiu, Y. G.; Suib, S. L.; O'Young, C. L. J. *Catalysis* **1994**, *150*, 34.

(5) Asensi, M. A.; Corma, A.; Martinez, A. *J. Catal.* **1996**, *158*, 561.

(6) Xu, W. Q.; Yin, Y. G.; Suib, S. L.; Edwards, J. C.; O'Young, C. L. *J. Phys. Chem.* **1995**, *99*, 9443.

(7) Oliver, F. G.; Munson, E. J.; Haw, J. F. *J. Phys. Chem.* **1992**, *96*, 8106.

(8) Xu, T.; Haw, J. F. *J. Am. Chem. Soc.* **1994**, *116*, 10188.

(9) (a) Aronson, M. T.; Gorte, R. J.; Farneth, W. E.; White, D. *J. Am. Chem. Soc.* **1989**, *111*, 840. (b) Haw, J. F.; Richardson, B. R.; Oshiro, I. S.; Lazo, N. D.; Speed, J. A. *J. Am. Chem. Soc.* **1989**, *111*, 2052. (c) Lazo, N. D.; Richardson, B. R.; Schettler, P. D.; White, J. L.; Munson, E. J.; Haw, J. F. *J. Phys. Chem.* **1991**, *95*, 9420.

(10) Malkin, V. G.; Chesnokov, V. V.; Paukshtis, E. A.; Zhidomirov, G. M. *J. Am. Chem. Soc.* **1990**, *112*, 666.

(11) Stepanov, A. G.; Zamaraev, K. I. *Catal. Lett.* **1993**, *19*, 153.

(12) (a) Kazansky, V. B. *Acc. Chem. Res* **1991**, *24*, 379. (b) Senchenya, I. N.; Kazansky, V. B. *Catal. Lett.* **1991**, *8*, 317. (c) Kazansky, V. B.; Senchenya, I. N. *J. Catal.* **1989**, *119*, 108.

(13) Viruela, P.; Zicovich-Wilson, C. M.; Corma, A. *J. Phys. Chem.* **1993**, *97*, 13713.

(14) Boronat, M.; Viruela, P.; Corma, A. *J. Phys. Chem.* **1996**, *100*, 633.

(15) (a) Hohenberg, P.; Kohn, W. *Phys. Rev. B* **1964**, *136*, 864. (b) Kohn, W.; Sham, L. J. *Phys. Rev. A* **1965**, *140*, 1133.

(16) (a) Parr, R. G.; Yang, W. In *Density Functional Theory of Atoms and Molecules*; Oxford University Press: New York, 1989. (b) Dreizler, R. M.; Gross, E. K. U. In *Density Functional Theory*; Springer: Berlin, 1990. (c) March, N. H. In *Electron Density Theory of Many-Electron Systems*; Academic Press: New York, 1991.

(17) Frisch, M. J.; Trucks, G. W.; Schlegel, H. B.; Gill, P. M. W.; Johnson, B. G.; Robb, M. A.; Cheeseman, J. R.; Keith, T.; Petersson, G. A.; Montgomery, J. A.; Raghavachari, K.; Al-Laham, M. A.; Zakrzewski, V. G.; Ortiz, J. V.; Foresman, J. B.; Cioslowski, J.; Stefanov, B. B.; Nanayakkara, A.; Challacombe, M.; Peng, C. Y.; Ayala, P. Y.; Chen, W.; Wong, M. W.; Andres, J. L.; Replogle, E. S.; Gomperts, R.; Martin, R. L.; Fox, D. J.; Binkley, J. S.; DeFrees, D. J.; Baker, J.; Stewart, J. P.; Head-Gordon, M.; Gonzalez, C.; Pople, J. A. *Gaussian 94*, Revision B.1; Gaussian: Pittsburgh, PA, 1995.

(18) (a) Becke, A. D. *J. Chem. Phys.* **1996**, *104*, 1040. (b) Bauschlicher, C. W., Jr. *Chem. Phys. Lett.* **1995**, *246*, 40. (c) Baker, J.; Muir, M.; Andzelm, J. *J. Chem. Phys.* **1995**, *102*, 2063. (d) Baker, J.; Andzelm, J.; Muir, M.; Taylor, P. R. *Chem. Phys. Lett.* **1995**, *237*, 53.

(19) Becke, A. D. *J. Chem. Phys.* **1993**, *98*, 5648.

(20) Perdew, J. P. *Phys. Rev. B* **1986**, *33*, 8822.

(21) Boronat, M.; Viruela, P.; Corma, A. *J. Phys. Chem.* **1996**, *100*, 16514.

(22) Hariharan, P. C.; Pople, J. A. *Chem. Phys. Lett.* **1972**, *16*, 217.

(23) Hariharan, P. C.; Pople, J. A. *Theor. Chim. Acta* **1973**, *28*, 213.

(24) Schlegel, H. B. *J. Comput. Chem.* **1982**, *3*, 214.

(25) (a) Gonzalez, C.; Schlegel, H. B. *J. Chem. Phys.* **1989**, *90*, 2154. (b) Gonzalez, C.; Schlegel, H. B. *J. Phys. Chem.* **1990**, *94*, 5523.

(26) (a) Moeller, C.; Plesset, M. S. *Phys. Rev.* **1934**, *46*, 618. (b) Binkley, J. S.; Pople, J. A. *Int. J. Quantum Chem.* **1975**, *9*, 229.

(27) (a) Sauer, J. *Chem. Rev. (Washington, D.C.)* **1989**, *89*, 199. (b) Sauer, J.; Ugliengo, P.; Garrone, E.; Saunders, V. R. *Chem. Rev. (Washington, D.C.)* **1994**, *94*, 2095.

(28) (a) Kazansky, V. B. *Acc. Chem. Res* **1991**, *24*, 379. (b) Kazansky, V. B. *Stud. Surf. Sci. Catal.* **1994**, *85*, 251.

(29) Corma, A. *Chem. Rev. (Washington, D.C.)* **1995**, *95*, 559.

(30) (a) Fan, L.; Ziegler, T. *J. Chem. Phys.* **1990**, *92*, 3645. (b) Baker, J.; Muir, M.; Andzelm, J. *J. Chem. Phys.* **1995**, *102*, 2063. (c) Deng, L.; Ziegler, T. *J. Phys. Chem.* **1995**, *99*, 612. (d) Jursic, B. S. *Chem. Phys. Lett.* **1996**, *256*, 213.

(31) Corma, A. Unpublished results.